

AD



Research and Development Technical Report ECOM-3575

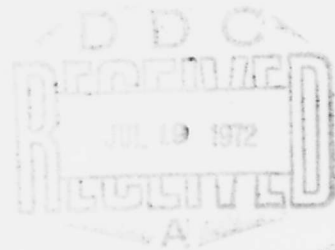
AD 745102

CONTROLLED HELICOPTER DISCHARGE

R.G. Buser
H.M. Kaunzinger
I. Gumeiner

May 1972

DISTRIBUTION STATEMENT
Approved for public release;
distribution unlimited.



ECOM

UNITED STATES ARMY ELECTRONICS COMMAND · FORT MONMOUTH, N.J.

Reproduced by
NATIONAL TECHNICAL
INFORMATION SERVICE
U S Department of Commerce
Springfield VA 22151

38R

Unclassified
Security Classification

DOCUMENT CONTROL DATA - R & D

(Security classification of title, body of abstract and indexing annotation must be entered when the overall report is classified)

1. ORIGINATING ACTIVITY (Corporate author) US Army Electronics Command Fort Monmouth, New Jersey 07703		2a. REPORT SECURITY CLASSIFICATION Unclassified	
		2b. GROUP NA	
3. REPORT TITLE Controlled Helicopter Discharge			
4. DESCRIPTIVE NOTES (Type of report and inclusive dates) Technical Report			
5. AUTHOR(S) (First name, middle initial, last name) Rudolf G. Buser Helmuth M. Kaunzinger Irwin Gumeiner			
6. REPORT DATE May 1972		7a. TOTAL NO. OF PAGES 30	7b. NO. OF REFS 11
8a. CONTRACT OR GRANT NO. a. PROJECT NO. ITO 61102 B31A c. Task No: 01 d. Work Unit No: 345		8b. ORIGINATOR'S REPORT NUMBER(S) ECOM - 3575	
8c. OTHER REPORT NO(S) (Any other numbers that may be assigned this report)			
10. DISTRIBUTION STATEMENT A proved for public release and sale, distribution unlimited			
11. SUPPLEMENTARY NOTES		12. SPONSORING MILITARY ACTIVITY Commanding General, USAECOM ATTN: AMSRL-TL-Q Fort Monmouth, New Jersey 07703	
13. ABSTRACT Several new approaches, potentially capable of discharging a helicopter to an operationally safe potential against ground, have been explored. Specifically, water spray discharges have been studied under various conditions and appear promising. Other elements of a complete active discharge system, namely, field sensor and information processor/indicator, have been developed and tested also, as well as the complete system itself.			

DD FORM 1473

REPLACES DD FORM 1473, 1 JAN 64, WHICH IS OBSOLETE FOR ARMY USE.

(1)

Unclassified
Security Classification

14. KEY WORDS	LINK A		LINK B		LINK C	
	ROLE	WT	ROLE	WT	ROLE	WT
Electrostatic charge Aircraft Electrostatic discharge Charge Transport Electrostatic Field Sensing						

Reports Control Symbol OSD-1366

TECHNICAL REPORT ECOM - 3575

CONTROLLED HELICOPTER DISCHARGE

by

R. G. Buser, H. M. Kaunzinger and I. Gumeiner

Quantum Electronics/Display Devices Technical Area
U. S. Army Electronics Technology and Devices Laboratory (ECOM)

May 1972

DA Work Unit No. 1T0.61102.B31A.01.345

DISTRIBUTION STATEMENT

Approved for public release;
distribution unlimited.

US Army Electronics Command
Fort Monmouth, New Jersey

ABSTRACT

Several new approaches, potentially capable of discharging a helicopter to an operationally safe potential against ground, have been explored. Specifically, water spray discharges have been studied under various conditions and appear promising. Other elements of a complete active discharge system, namely, field sensor and information processor/indicator, have been developed and tested also, as well as the complete system itself.

CONTENTS

	<u>Page</u>
1. PROGRAM OBJECTIVE	1
2. OVERALL SYSTEMS CONCEPT	1
3. THE DIELECTRIC DISCHARGE (PASSIVE AND ACTIVE)	1
3.1 Theoretical Considerations	1
3.2 Experimental Approach and Experimental Results	4
4. ELECTRIC FIELD SENSING	20
4.1 Corona Discharge Noise Indicator	22
4.2 Electrostatic Field Sensing Methods	22
5. INFORMATION PROCESSOR/INDICATOR	24
6. OVERALL SYSTEM TESTS	26
7. FUTURE EXPERIMENTS	28
8. SUMMARY	29
9. ACKNOWLEDGEMENTS	29
10. REFERENCES	29

FIGURES

	<u>Page</u>
1. Helicopter discharge system.	2
2. Helicopter air circulation pattern.	5
3. Setup for discharge experiments.	6
4. Laser triggered remote control circuitry.	8
5. Comparison of ohmic discharge with large droplet discharge.	9
6. Discharge rate comparison for different heights and initial voltages U_0 .	11
7. Time dependence of tank pressure and fluid emission.	12
8. Comparison of dual nozzle with single nozzle.	13
9. Comparison of antifreeze with water.	15
10. Modified setup for reduced effective resistance.	16
11. Oscilloscope display of helicopter voltage and discharge current.	17
12. Active discharge from a nozzle within a constant electric field.	19
13. Effect of biased electrode on spray discharge rate.	21
14. Circuit diagram of the signal sensor triggered discharge control.	25
15. Suspended fuselage.	27

CONTROLLED HELICOPTER DISCHARGE

1. PROGRAM OBJECTIVE

Long range objective is to develop a technically sound, economical, and operationally acceptable system which permits an automatic discharge of the helicopter to zero potential between cargo hook (or helicopter) and ground during loading operations. Previously, it had been established that existing methods, such as the active corona discharge and the passive wick discharge, were severely limited in performance¹ (current limited; recirculation problem), or, as in the case of the resistive link,² operationally not acceptable. Various proposals for other schemes have been recently analyzed, such as laser induced breakdown, radioactive discharge, and chemical discharge; in all cases, the prospects for successful operation do not look promising.³ Objective of this one-year in-house program was to develop new ideas to the solution of the problem, select the more promising avenues for analysis, and perform an actual theoretical and experimental feasibility study for the most promising cases. Results of this work are discussed in sections 3, 4, 5, and 6.

2. OVERALL SYSTEM CONCEPT

During the initial phases of the program study, it became increasingly clear that operational constraints are just as important as the technology and physics of a given approach. The operational approach, which we propose to follow, assumes that the helicopter proceeds from ground and follows its mission irrespective of what happens to its charge (a discharge during flight is only considered if radio interference becomes critical), until the location for loading or unloading, etc., is reached. At this point in our technical approach, a field sensor located on the hook determines field strength and polarity and transmits the information to the discharger. When the field is excessive, the discharge takes place while a red warning light indicates danger. When the field is near zero, a green safety signal appears and the discharger is turned off. The helicopter is now for a given time (which depends on meteorological conditions, usually a few seconds) very close to ground potential. The principal elements of the system are shown in Fig. 1, and consist of a field sensor, an information receiver and processor, indicator lights, and most important, the discharger. Quite appropriately, during the work to be discussed, more effort was expended on the discharge mechanism and field sensor on which the performance of the overall system depends critically.

3. THE DIELECTRIC DISCHARGE (PASSIVE AND ACTIVE)

3.1 Theoretical Considerations

The approach selected to study the discharge of the helicopter, one may call a dielectric discharge method. If a helicopter emits a water beam towards ground, one might, at first sight, expect an ohmic connection

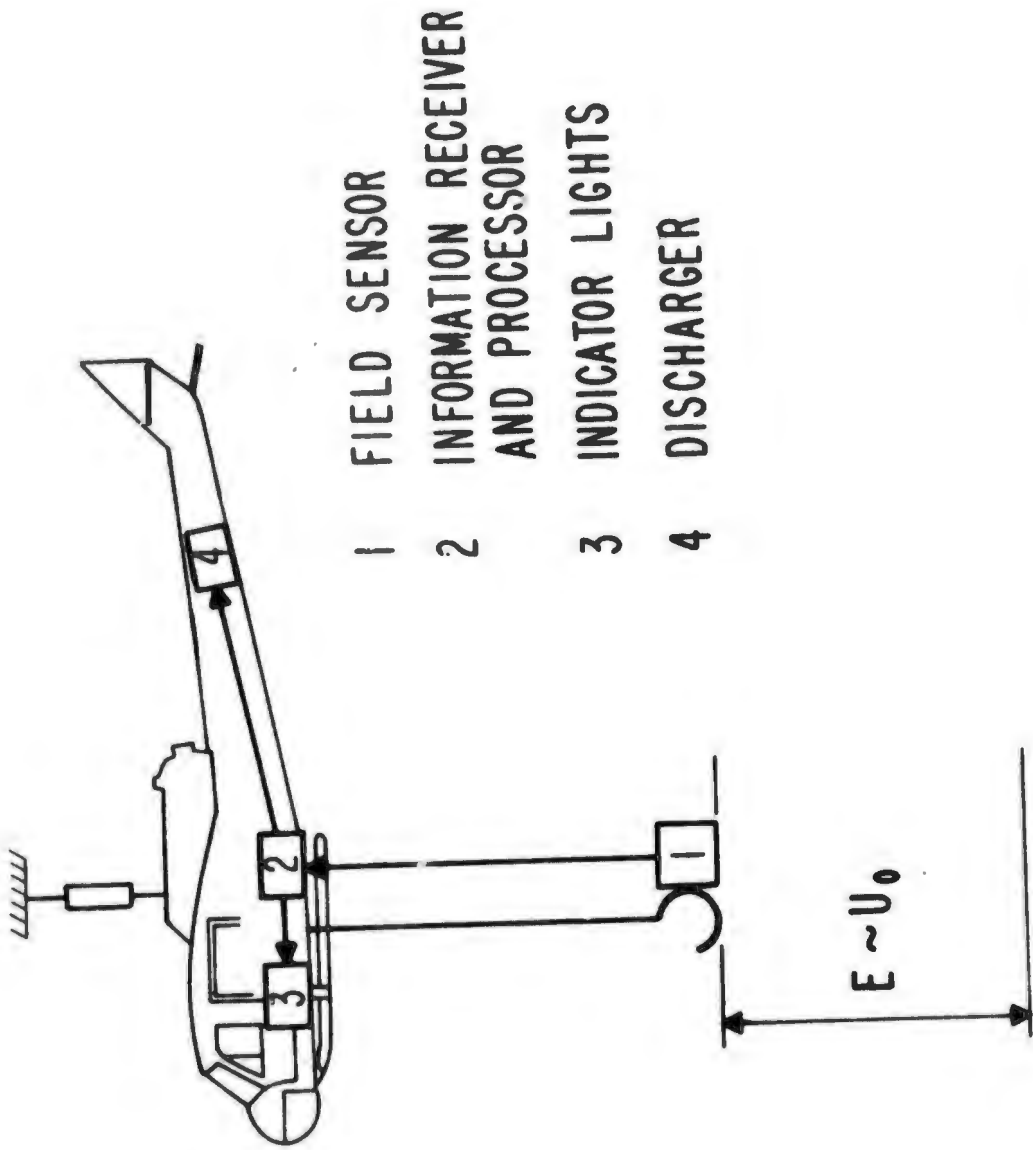


FIG.1 HELICOPTER DISCHARGE SYSTEM

to ground with a resistance in the order of $10^6 \Omega$. This assumption implies a discharge current approximately 0.05A produced by a typical voltage of 50 kV during a time in the order of 1 millisecond (ms) (magnitude of discharge time constant is $\tau = RC \approx 10^6 \times 10^{-9} = 10^{-3}$ seconds). A current of this value is hazardous to the human body.⁴ However, even without air circulation, the emitted water column is broken up after a short distance into isolated air droplets of varying size, and each droplet may carry a certain amount of charge. In the extreme case, a nozzle producing a spray mist may be used.

The charge of an individual droplet is

$$q \sim \epsilon_0 u r \quad (1)$$

and the discharge current

$$I(t) = u(t)/R_e(t) = Nq \sim \epsilon_0 u(t) \bar{r}(t) N(\bar{r}, t), \quad (2)$$

with q = charge, u = effective voltage, ϵ_0 = dielectric constant, r = radius of droplet, N = number of droplets per time unit, R_e = effective resistance (bar indicates average). Estimates, as discussed later, yield R_e values between 10^9 and $10^{10} \Omega$; therefore, τ is in the order of a second, and I_{max} in the microampere range. Note that the material and its conductivity below the surface of the sphere are of no significance in this approximation. This seems to indicate that water surface being the same, water bubbles should perform as well as solid droplets, a potential aspect for reducing material consumption.

Equation (2) permits the following modes of operation:

a. Passive Discharge

The effective voltage $u(t)$ in Equation (2) is related to the helicopter-to-ground voltage and produces a proportional discharge current $I(t)$. Assuming a constant flow rate of discharge liquid and uniform droplet size and distribution, $u(t)$ and $I(t)$ decay at an exponential rate. Therefore, the discharge to a safe voltage level will take excessive time when the initial voltage U_0 is orders of magnitude higher than this safe level.

b. Active Discharge⁵

The effective voltage $u(t)$ in Equation (2) is kept constant as

a high voltage bias is applied to a charge inducing electrode in front of the nozzle. The effective electrostatic field at the nozzle orifice is also much higher than in the passive discharge case where the charge inducing field originates from the relatively remote ground. As a result, the discharge current $I(t)$ is theoretically constant and much higher than in the passive discharge case. Therefore, the discharge will approach the safe level as a steep linear function of time and will be completed much sooner than with the passive method.

At the present time, we have not established the limitations in the choice of R . If we assume, for example, N in the order of 10^8 , each drop of 100 micron size, and a charge of $10^8 \times 1.6 \times 10^{-19}$ coulomb per drop, we find $I = 16 \mu A$.^{*} There exists little information⁶ on this subject and available information is to be taken with reservation.

It is recognized that these estimates may have to be considerably modified in actual helicopter field environment. A study of the air circulation pattern indicates that successful operation of the discharge may critically depend upon optimal positioning of the dielectric discharge on board the helicopter.

Figure 2 shows the air flow pattern created by the rotating blades. Taking advantage of this pattern, positioning of spray nozzles at the vortices of both low turbulence profile cones is essential in order to avoid detrimental recirculation of charges. Placing the discharge source into the turbine propulsion flow field appears also advantageous. However, a compromise in positioning must be made, as the stream velocity distribution calls for attachment close to the turbine jet hole while the stream temperature distribution prohibits locations in the immediate vicinity.

3.2 Experimental Approach and Experimental Results

In order to appropriately simulate the discharge of a helicopter (avoiding the scaling problem), a complete fuselage of a UH1C helicopter with landing skids (but without main and tail rotors) has been suspended (using an extremely low leakage insulator) from a crane inside hangar #5 at the N.A.S.** at Lakehurst, N.J. Fire extinguisher tanks with a 2.5 gallon capacity each, were mounted to this fuselage with the nozzle assembly level with the skids. Before each experiment, these fire extinguishers were removed, weighed, filled with $2\frac{1}{2}$ gallons of discharge fluid (usually tap water), weighed again, charged to a starting pressure of 100 lb and mounted again. Figure 3 shows a diagram of the setup. An instrumentation van contained the variable high voltage power supply with reversible polarity, a Keithley electrometer of the type 610 B (input impedance $\approx 10^{14} \Omega$), and a Hewlett Packard chart recorder. The suspended helicopter shell was connected to the high voltage power supply through a $10^7 \Omega$ current limiting

^{*}Laboratory experiments showed that a single spray nozzle can produce a discharge current in excess of $15 \mu A$ under optimized conditions.

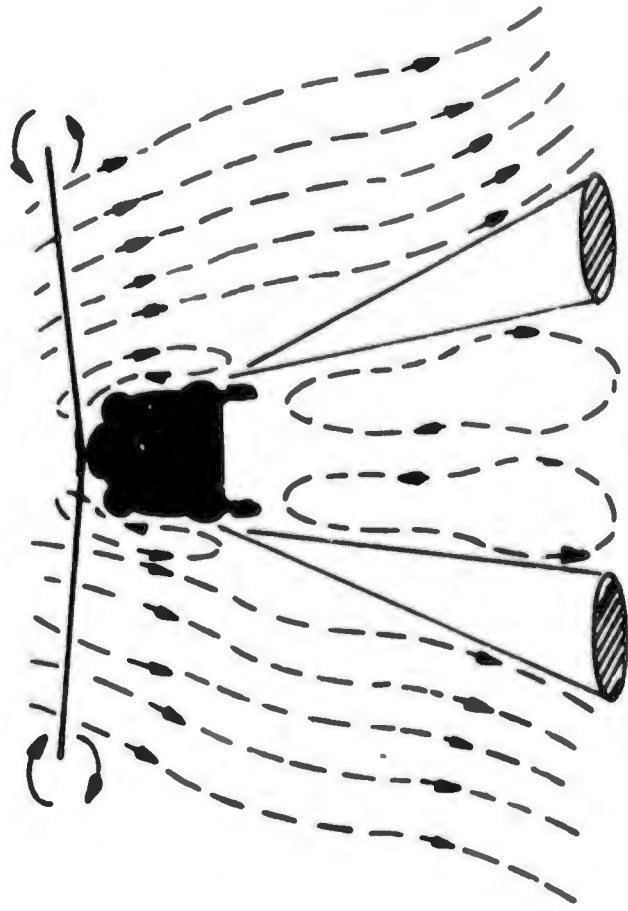


FIG.2 HELICOPTER AIR CIRCULATION PATTERN

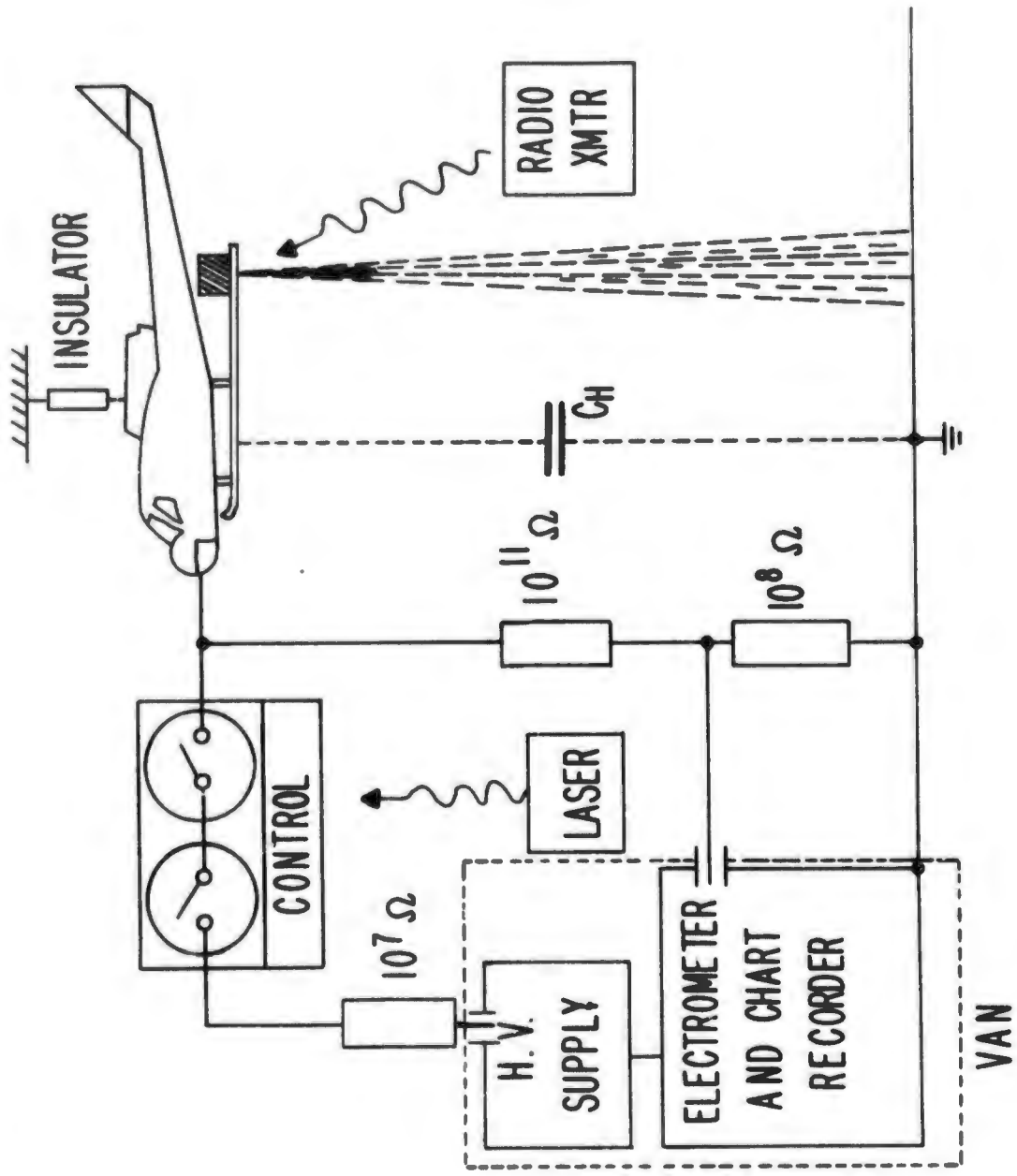


FIG.3 SETUP FOR DISCHARGE EXPERIMENT

resistor and two vacuum contactors manufactured by Jennings Radio. The two vacuum contactors were connected in series in order to keep the combined leakage resistance above $10^{11} \Omega$ up to 50 kV. Their control circuitry is located on a floating subchassis and utilizes two photosensitive resistors (one for "on," one for "off") controlling digital amplifier circuitry and coils for the high voltage relays, all battery operated. When one of the photosensitive resistors is illuminated from below with a laser beam, the corresponding open or closed position of both relays is triggered. Details of the circuit diagram are shown in Fig. 4.

The suspended helicopter fuselage is also connected to a 1000:1 resistive divider with a total resistance of $10^{11} \Omega$ for voltages up to 100 kV. The $10^6 \Omega$ tap is in parallel with the input of the Keithley electrometer which feeds the HP chart recorder. The capacitor C_H in Fig. 3 denotes the total effective capacitance between the helicopter fuselage and ground.

The actual helicopter capacitance C_H , for a distance of 10 ft between ground and skids, has been determined by charging the fuselage to -20 kV, opening the vacuum contactors, and discharging the fuselage through the $10^{11} \Omega$ resistive divider. With both C_H and the equivalent discharge resistance R_D independent of voltage and time, this discharge follows the relationship

$$u = u_0 \exp(-t/R_D C_H)$$

The recording of this decay, taken with the HP recorder, has been plotted on single logarithmic paper as a straight line. It is shown as curve B in Fig. 5 indicating a time lapse of 44.3 seconds for a 2.72 to 1 voltage decay. The resulting effective capacitance at 10 ft height is:

$$C_H = 443 \times 10^{-12} \text{ F}$$

This relatively high value probably results from additional stray capacitances caused by the leads to the resistive divider and to the vacuum contactors, and by the proximity of one hangar side wall and the boom of the crane. A more realistic capacitance of the fuselage (10 ft height) to ground is near 400 pF. However, for all successive tests, the existing capacitance of 450 pF was used for assessment of the equivalent resistances of the various discharge methods applied.

The following modes of fluid discharge have been explored:

- a. Passive droplet beam (large average drop size),
- b. Active droplet beam with electrostatic bias (large average drop size),

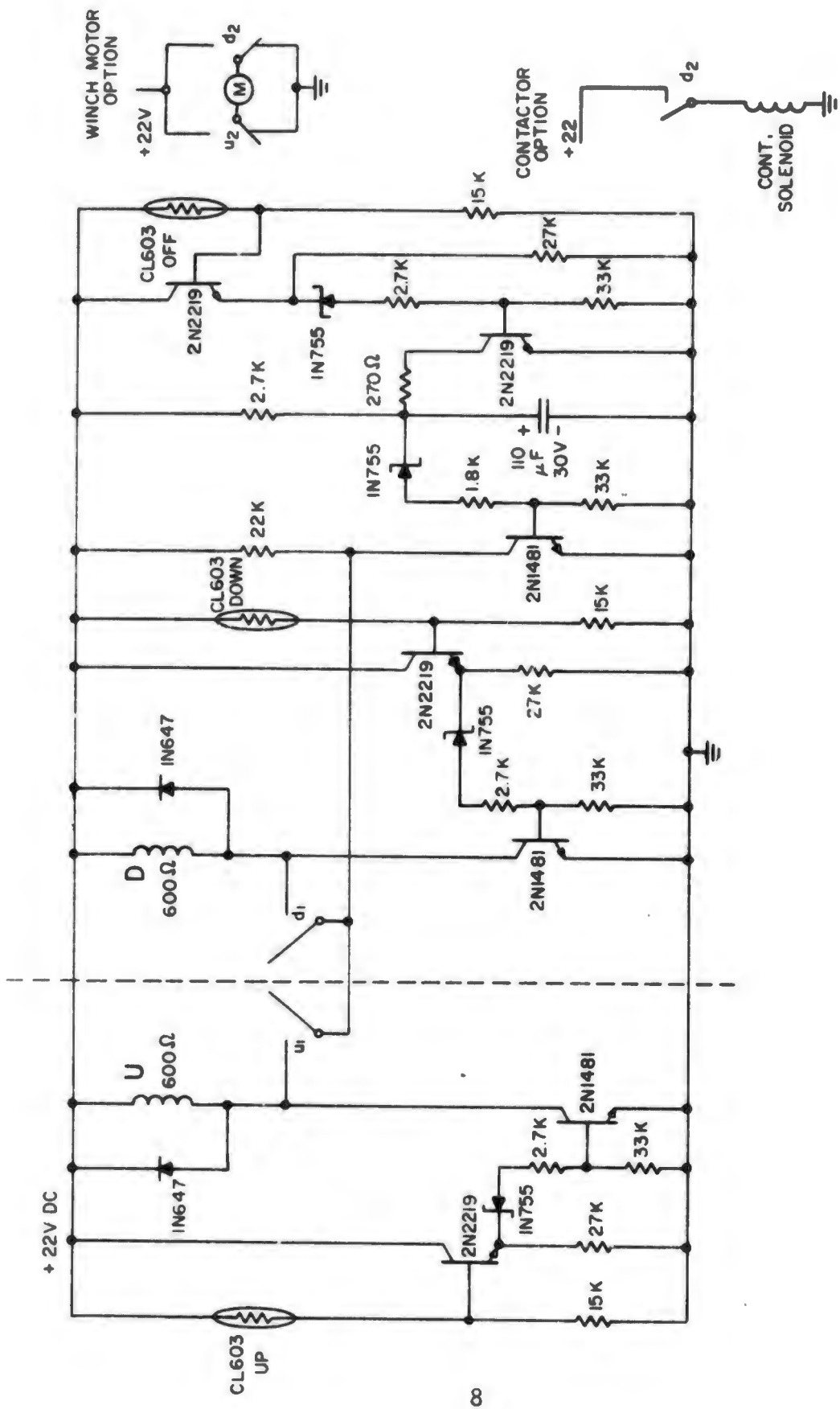


FIG. 4 LASER TRIGGERED REMOTE CONTROL CIRCUITRY

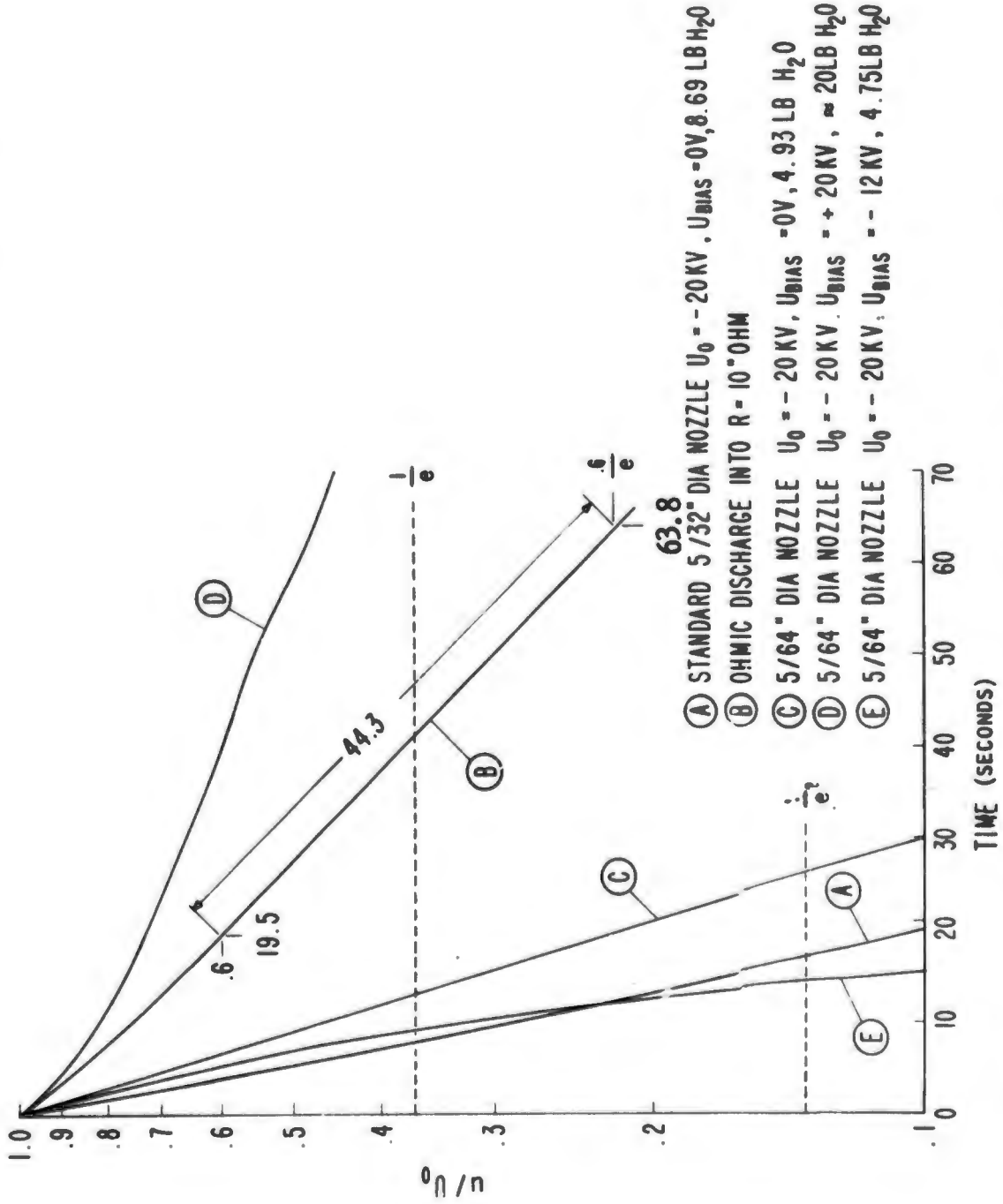


FIG. 5 COMPARISON OF OHMIC DISCHARGE WITH LARGE DROPLET DISCHARGE

- c. Passive fluid spray (small average drop size),
- d. Active fluid spray with electrostatic bias (small average drop size).

In case a and b, the droplet beam was initially confined into a narrow and continuous jet where visible breakup in individual drops takes place after 1 to 2 ft of downward travel. This initially narrow beam is a result of the constant diameter orifice with a length to diameter ratio of 2 to 1. This type nozzle with an orifice diameter of $5/32''$ is subsequently referred to as "standard nozzle." Figure 6 shows the discharge obtained with tap water and a single beam from this standard nozzle. In this and all subsequent discharges, the following simultaneous operations coincide at zero time: opening of contacts between high voltage supply and fuselage by laser beam control; opening of the magnetic valve between the fluid storage tank and nozzle by radio control; and return of the disconnected high voltage supply to zero volts. The plots in Fig. 6 show results of the passive helicopter discharge with tap water at -20 kV and -50 kV initial voltage, each at 10 and 20 ft height of the skids above ground. The indicated quantities of water on the graph show the total amount of water needed for a discharge from -20 kV or -50 kV to -2kV. At 37% ($1/e$) of the initial voltage, the equivalent resistance is $1.75 \times 10^{10} \Omega$ for 10 feet height and $2.2 \times 10^{10} \Omega$ for 20 ft height, independent of the initial charge level. Adding 4 oz of table salt to each gallon of water, and repeating these experiments, did not affect the discharge rate. The inference is that the electrical discharge takes place by charge carrying drop surfaces rather than by conduction of the liquid electrolyte. In a separate test on the ground, the tap water used and the pressure drop for the particular 2.5 gallon fire extinguisher pressure tank was determined as a function of time and plotted in Fig. 7. The water flow through the standard nozzle (as expected) is almost linear with time and allows a reasonably accurate interpolation of fluid dispersed as a function of voltage drop during the helicopter discharge. A comparison of discharge rates of single versus dual standard nozzle is shown in Fig. 8. This graph should show a 2 to 1 reduction in

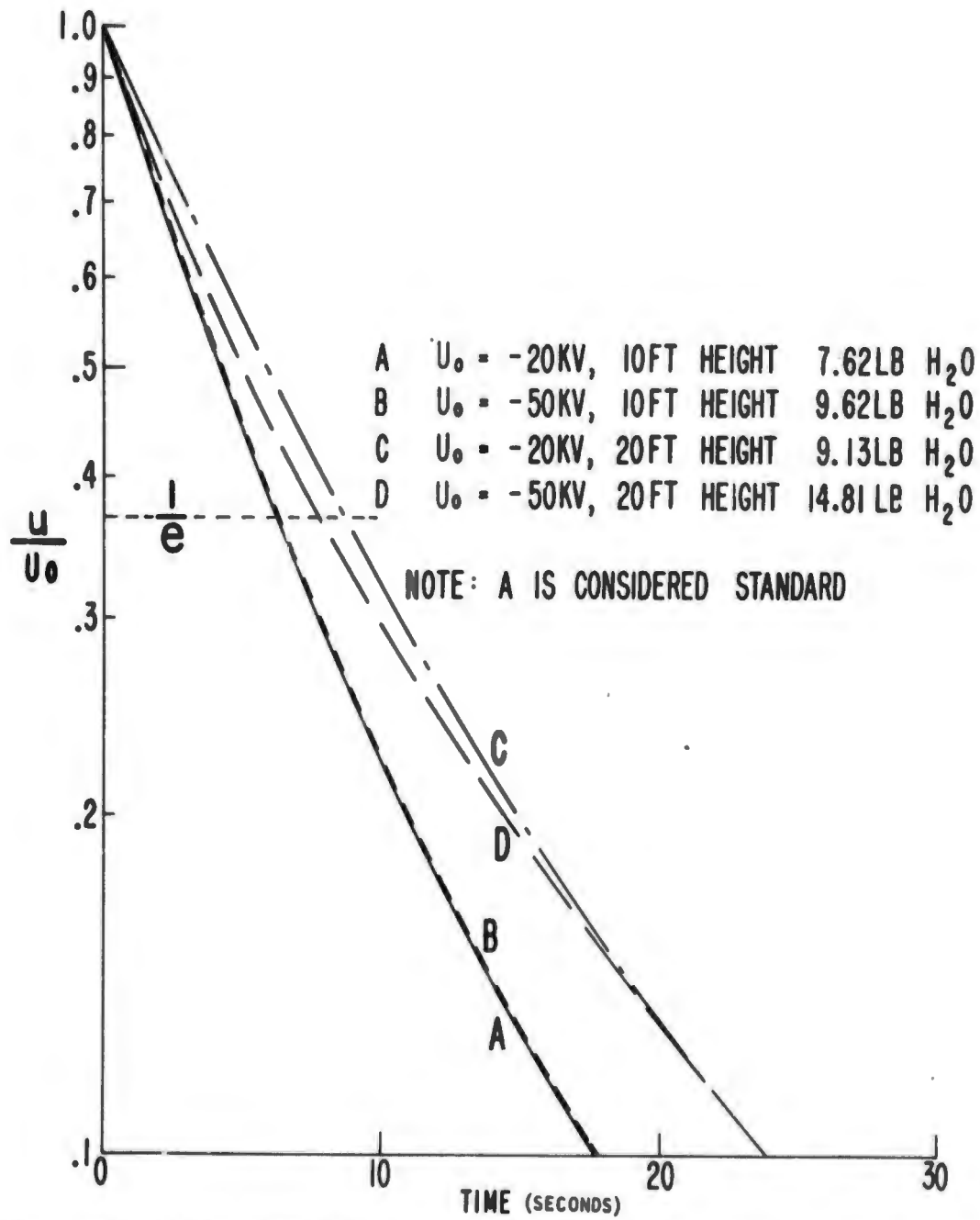


FIG. 6 DISCHARGE RATE COMPARISON FOR DIFFERENT HEIGHTS AND INITIAL VOLTAGES U_0

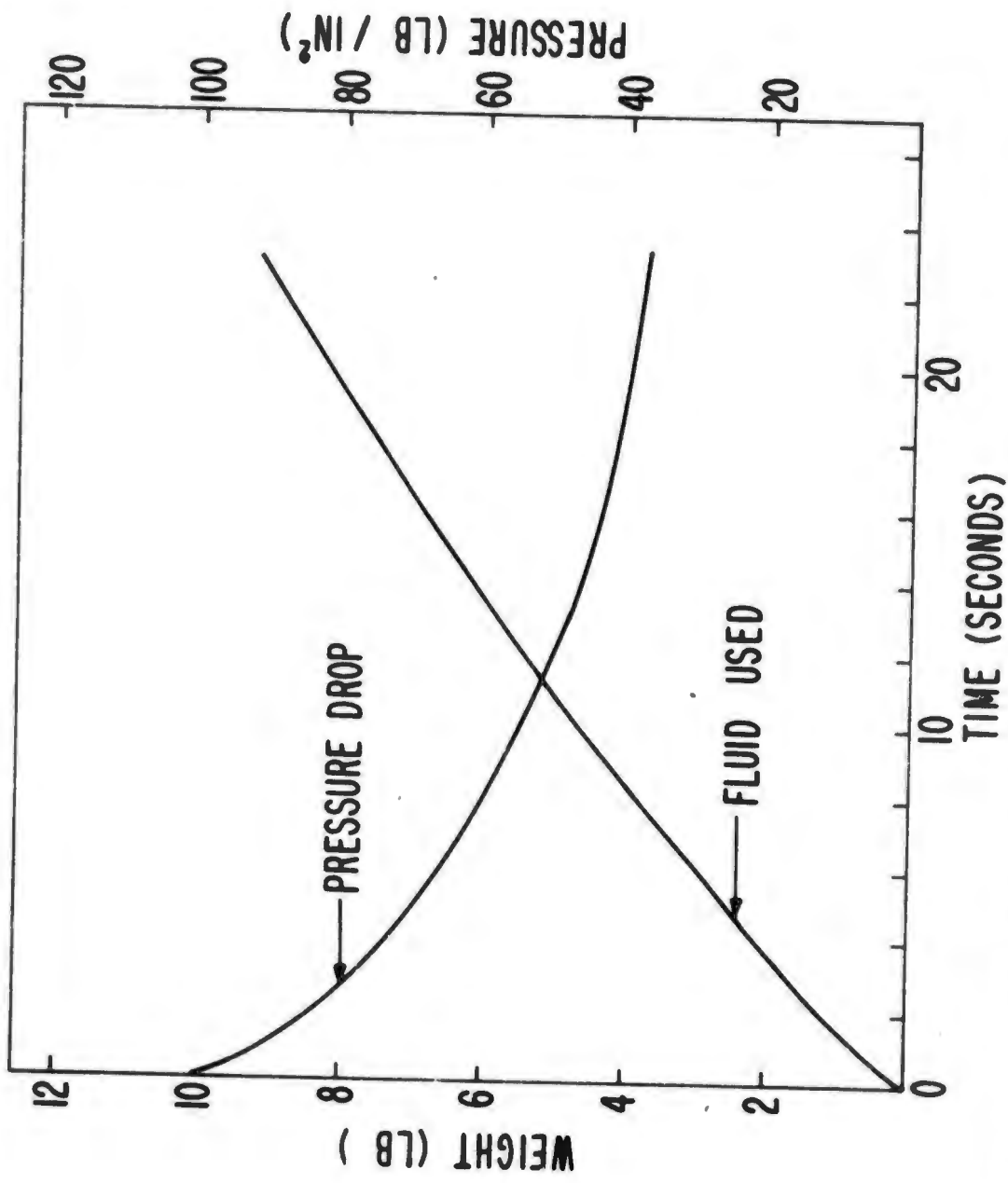


FIG.7 TIME DEPENDENCE OF TANK PRESSURE AND FLUID EMISSION

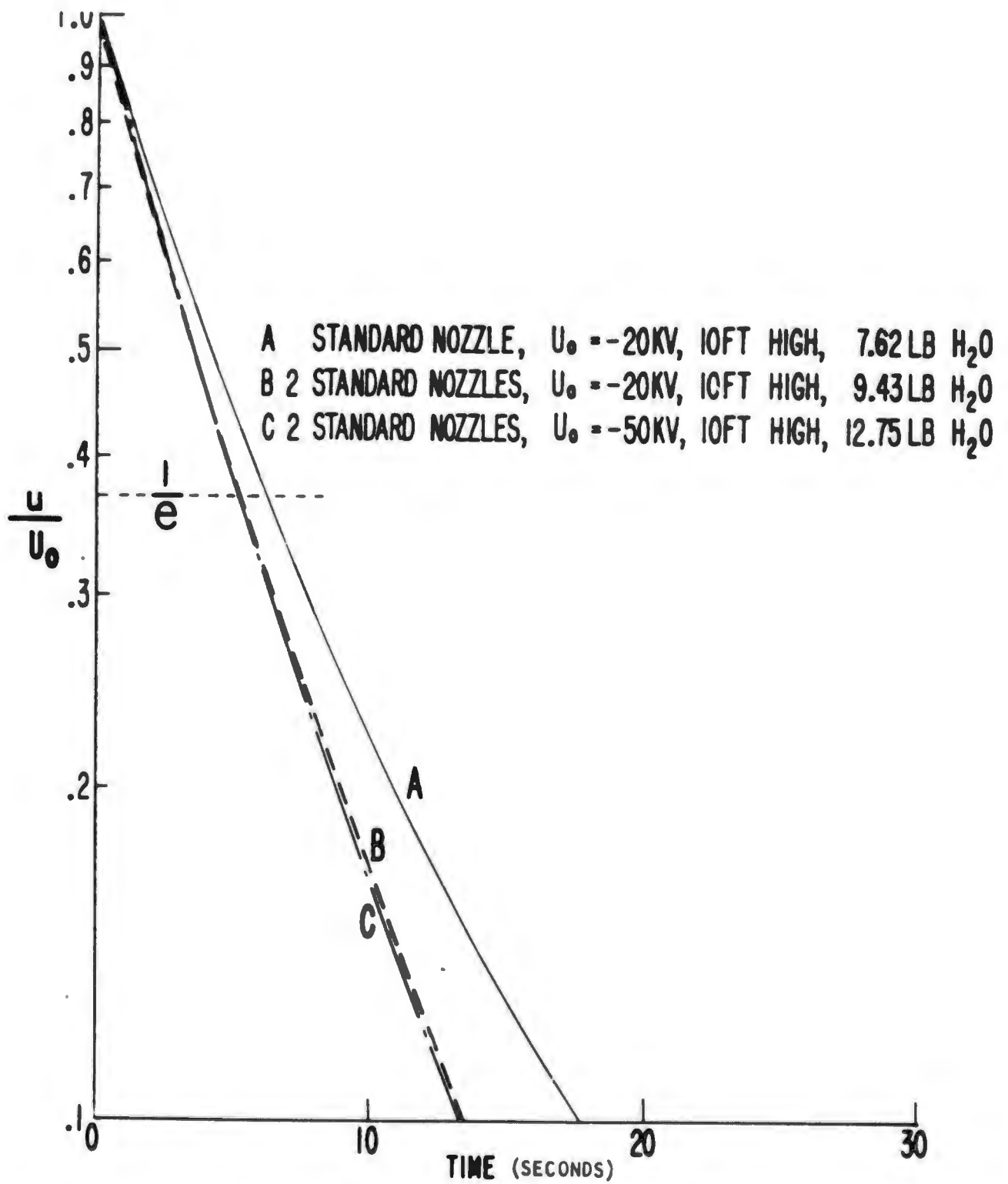


FIG. 8 COMPARISON OF DUAL NOZZLE WITH SINGLE NOZZLE

discharge time for the same voltage discharge ratio because of the expected two-fold amount of charge carrying drops. However, the fluid dispensed from the two pressure tanks was not equal due to a difference in flow restriction imposed by the individual magnetic valves between tanks and nozzles. Actually, one tank dispensed twice as much water as the other one. The equivalent discharge resistance for the two tanks has dropped to $1.3 \times 10^{10} \Omega$ for the 10 ft height, and is again independent from the initial helicopter charge. It is obvious that the concept of a multiple nozzle system and its independent operation may be quite important.

Considering the wide temperature range for military operations, antifreeze (ethylene glycol of purity as per MIL Specs) has been used instead of water in some experiments. This comparison, using the standard nozzle from 10 ft height, is shown in Fig. 9 and indicates little difference in discharge rate between antifreeze and water. An expansion of this comparison to a mixture of 50% H₂O and 50% ethylene glycol did not reveal any significant changes and the plot is omitted.

All electrostatic discharges, with fluids described so far are of the passive droplet beam type, resemble (in the first approximation) the behavior of a constant resistor and have the disadvantage of reaching zero charge after a theoretically infinite time. All tests show no apparent discharge dependence on the charge polarity.

It was of interest, after these tests, to measure the resistance of water and ethylene glycol confined in a plastic hose of $\frac{1}{4}$ inch inside diameter and 12 ft length. Because of the expected lower resistance of this discharge path, the discharge time constant would be smaller than the time constant of the distributed capacitances and resistances of the $10^{11} \Omega$ voltage divider assembly. Therefore, it was expected to obtain a qualitative observation of dynamic charge distribution changes on the fuselage extremities during the discharge. The test setup was modified for this particular discharge through a liquid column and is shown in Fig. 10. Each switch symbol means a Jennings vacuum contactor. The trigger input of the oscilloscope was taken from the solenoid of the contactor located between the lower end of the hose and the $10^4 \Omega$ viewing resistor. Figure 11 shows the behavior of the $\frac{1}{4}$ " diam water column. The left portion of the upper trace shows approximately 16 kV of initial helicopter voltage (20 kV setting of high voltage control is more accurate). The right portion of the upper trace shows the helicopter approaching zero volts after

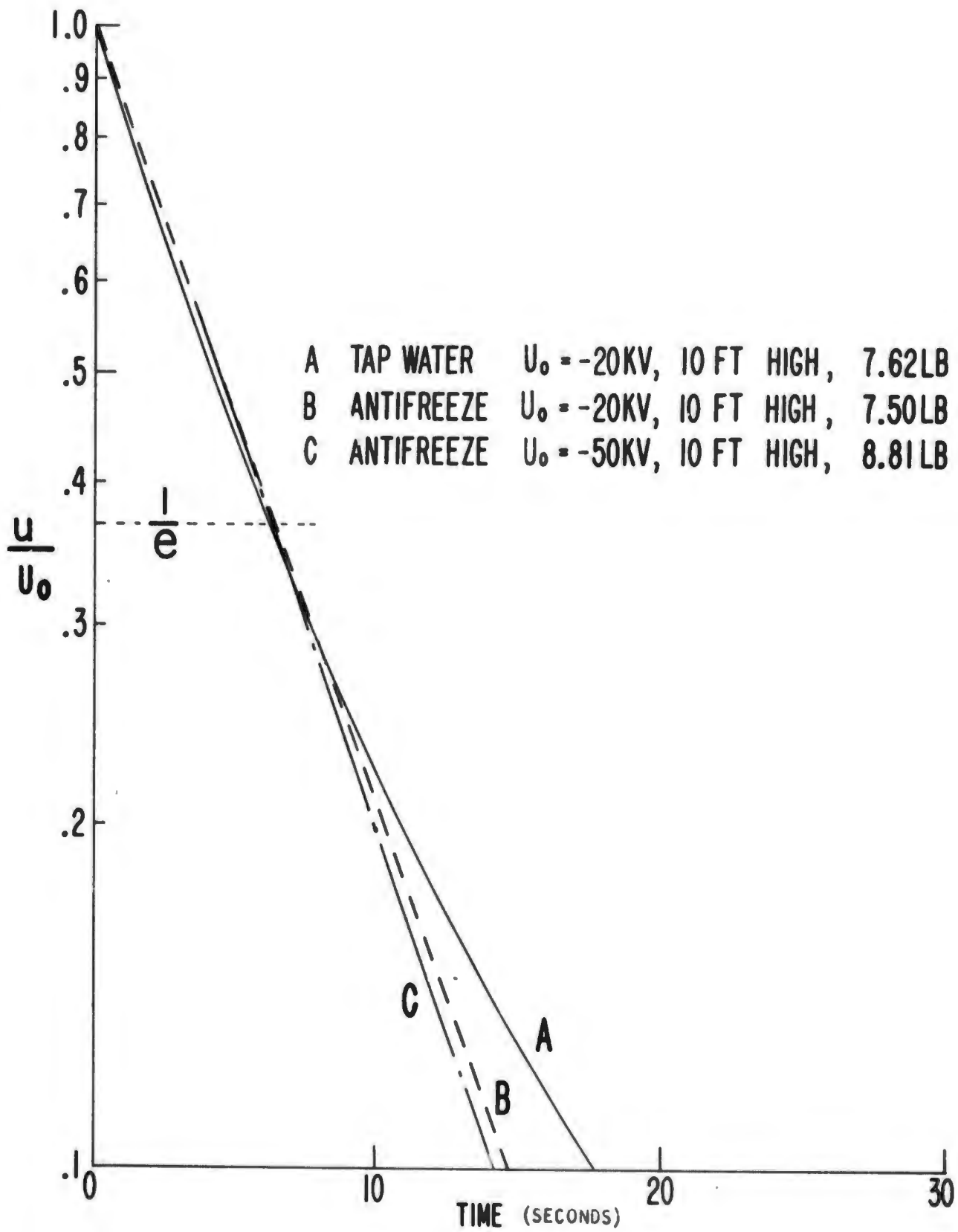


FIG.9 COMPARISON OF ANTIFREEZE WITH WATER

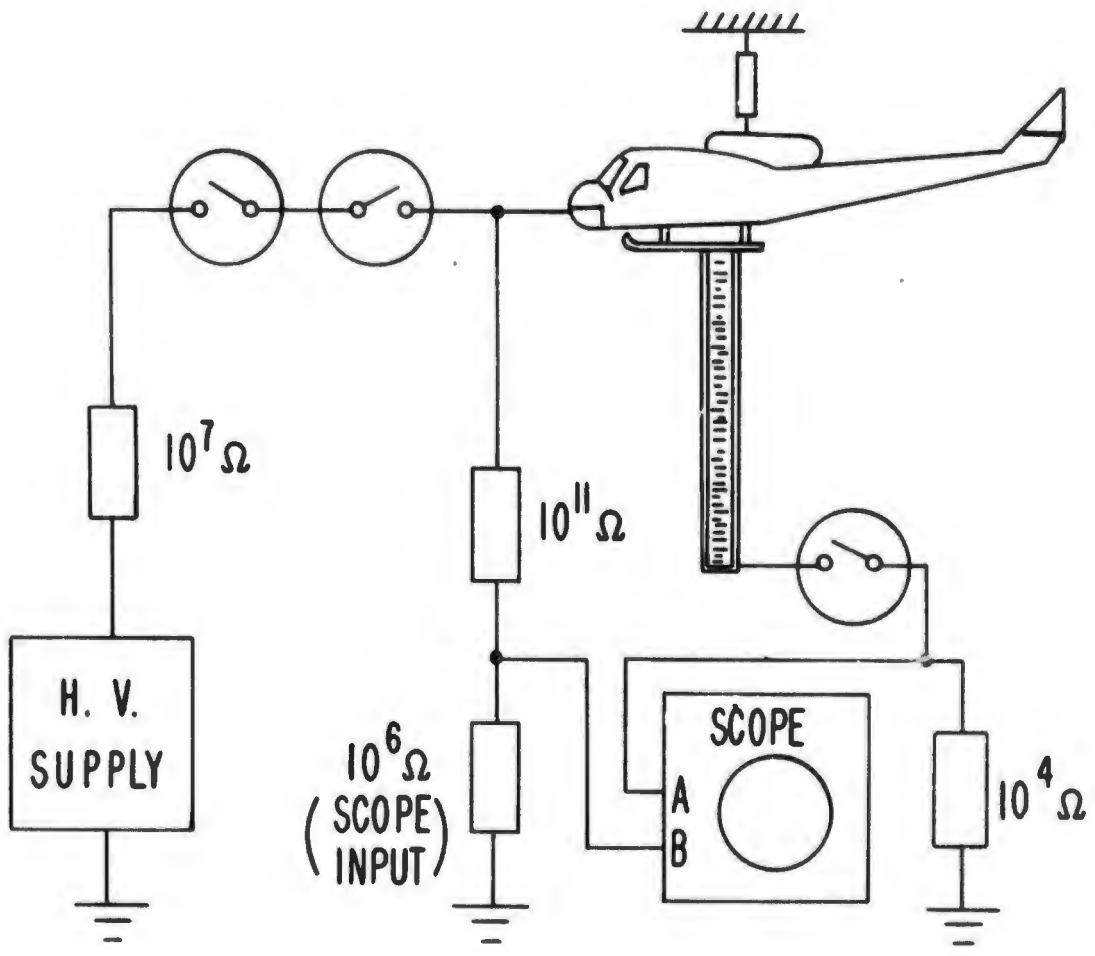


FIG.10 MODIFIED SETUP FOR REDUCED EFFECTIVE RESISTANCE

NOTE: Horizontal 20 ns/cm
Vertical Upper 20 kV/cm
Vertical Lower 20 μ A/cm

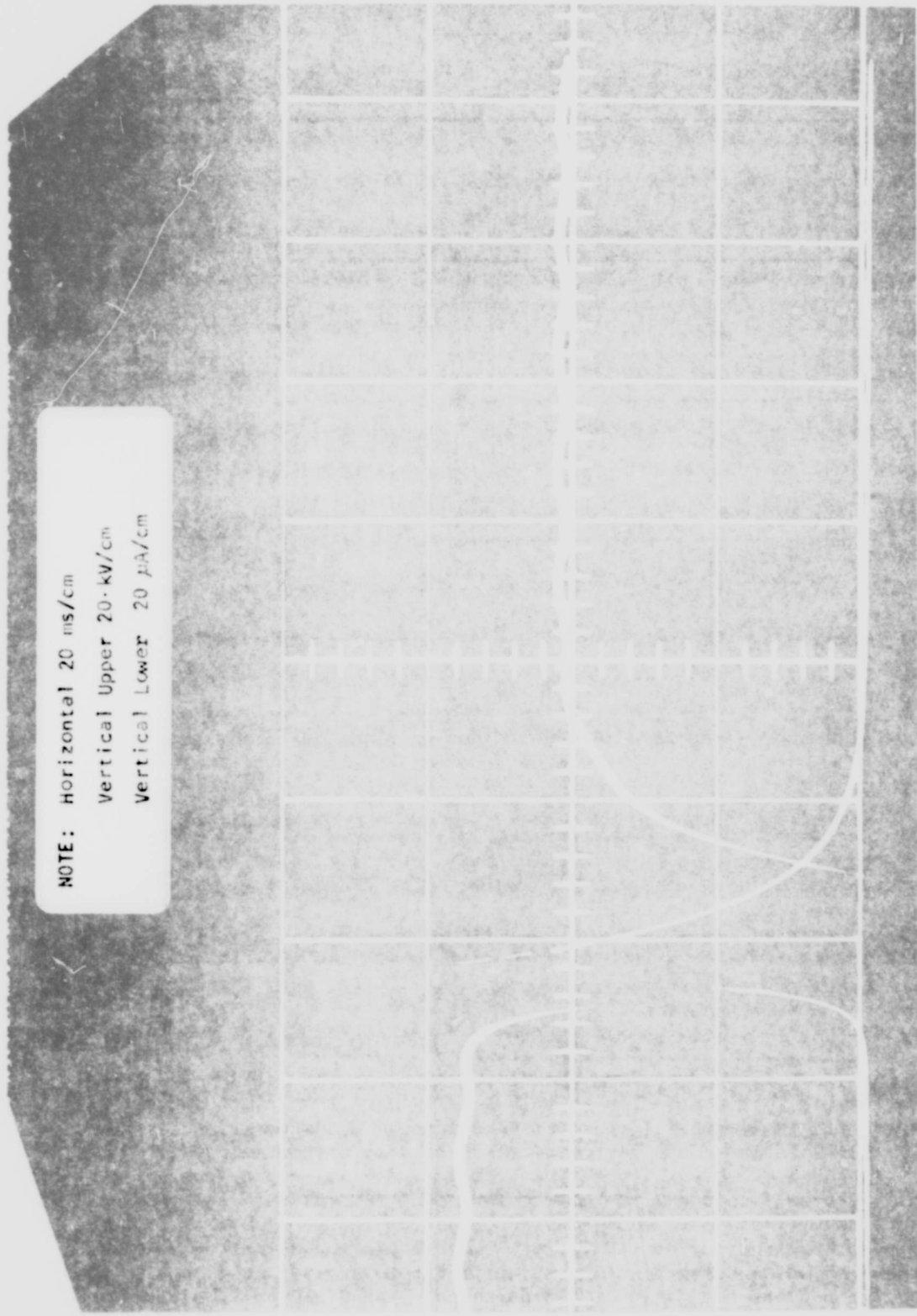


FIG.11 OSCILLOSCOPE DISPLAY OF HELICOPTER VOLTAGE AND DISCHARGE CURRENT

the discharge. The voltage pulse reaching below the coordinates during the discharge period is very important for this experiment. It indicates a significant temporary shift of charges from the resistive divider location to the location of the discharge hose during the discharge time, before the total charge on all helicopter extremities is redistributed again after reaching equilibrium. The lower trace shows the hose discharge current as a function of time and reveals a decay time constant of approximately 6 ms. The resulting effective resistance of this 12 ft long water column of $\frac{1}{4}$ " diam is $1.35 \times 10^7 \Omega$, three orders of magnitude below the effective resistance of the water beam from the standard nozzle at a 10 ft height. In the same way, we derived for the antifreeze a column decay time constant of approximately 1 ms and computed the approximate effective resistance of the 12 ft long $\frac{1}{4}$ " diam antifreeze column to $2.2 \times 10^6 \Omega$, almost four orders of magnitude below the effective value for the standard nozzle antifreeze beam from a 10 ft height.

In an effort to overcome the asymptotic approach towards zero helicopter voltage inherent with the large droplet fluid beam, an electrostatic bias was applied to a ring shaped electrode of 1 inch inner toroidal diameter concentric with the tip of the standard nozzles.⁵ This arrangement is shown in Fig. 12. The constant bias of this ring now mainly determines the discharge mechanism independent of the helicopter - ground potential. Thus, a feedback in the control system is possible which permits a controllable discharge of the helicopter.

In comparison to the numerous passive large droplet beam results, less data for the active large droplet beam have been taken during the period covered by this report. All active large droplet beam data have been obtained with a nozzle with the standard 2 to 1 orifice length to diameter ratio having a $5/64$ inch diam orifice. Results are plotted in Fig. 5 (line marked E) in comparison to the ohmic discharge (Load $10^{11} \Omega$) and to the passive beam case. As it turns out, the bias polarity against the nozzle tip must be the same as the voltage polarity of the fuselage against ground (this is in distinction to the small droplet case to be discussed later). With a bias of -12 kV for example, the discharge from the -20 kV level to the -2 kV level can be accelerated by a factor 2 with only one-sixth of the water used as compared with the passive fluid discharge case. The actual time between the initial -20 kV level and zero crossing was 16 seconds (water consumption 0.8 lb). When the bias polarity is reversed, while the polarity of the fuselage with respect to ground remains unchanged, the droplets leaving the nozzle now carry charges of the wrong polarity and tend to enhance the helicopter charge. The resulting helicopter voltage response, shown as curve D in Fig. 5, reflects this reversed charge transport which opposes the ohmic discharge through the $10^{11} \Omega$ voltage divider and causes a much slower voltage decay.

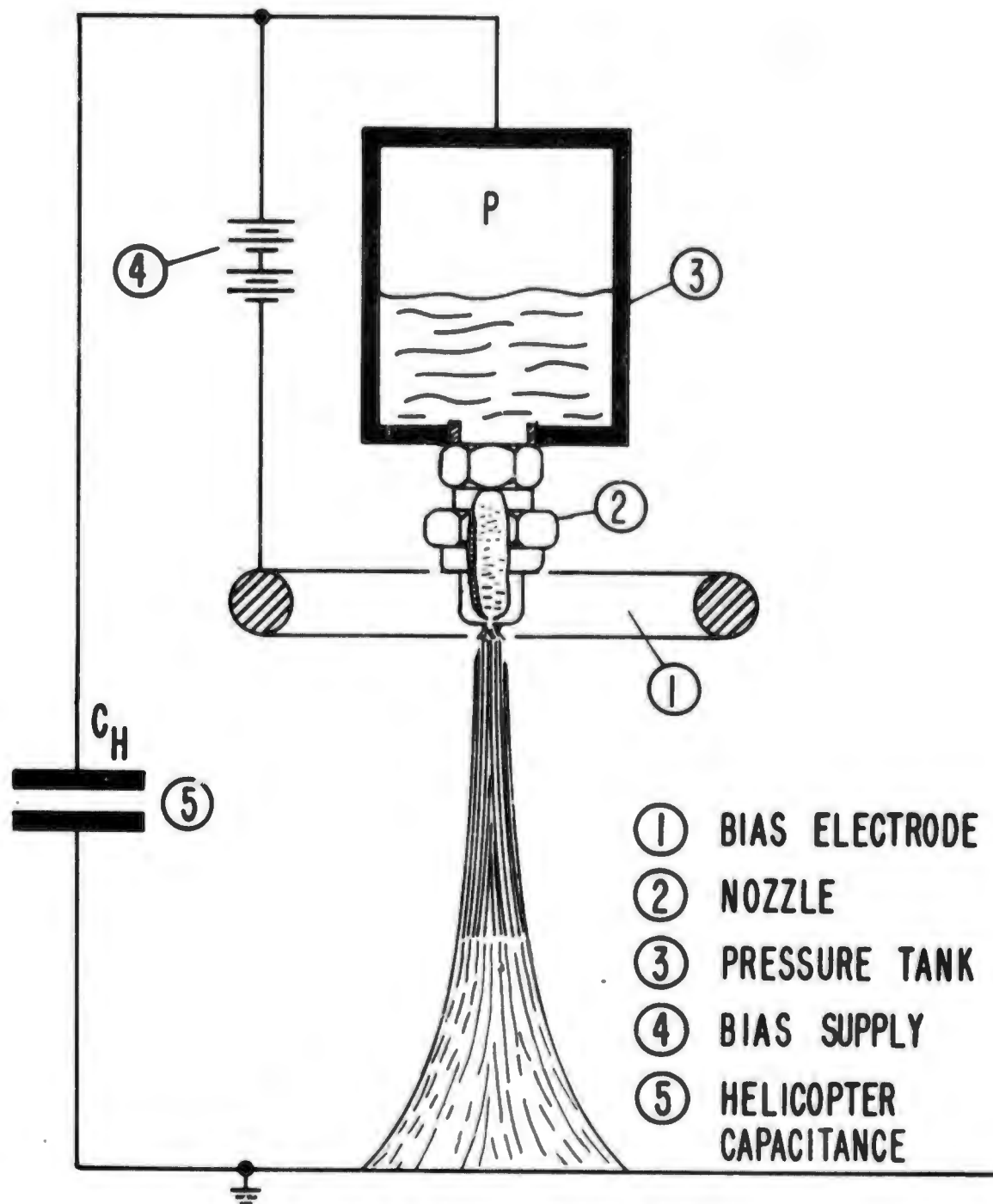


FIG.12 ACTIVE DISCHARGE FROM A NOZZLE WITHIN A CONSTANT ELECTRIC FIELD

The high voltage supply used for biasing the nozzle is located on the helicopter and is operated from the batteries mounted inside the fuselage. Since no battery operated high voltage supply was available, a television flyback transformer was modified with a low impedance primary and driven with high power transistors in push-pull operation to generate high ac voltage at a frequency of approximately 16 kHz. The secondary, made up from all original windings, provided enough peak-to-peak voltage to obtain up to 20 kV dc with a diode doubler circuit.

To study small droplet sprays, several spray nozzles were adapted and mating bias electrodes built before arriving at the first useful construction. The exterior arrangement was similar to the one shown in Fig. 12. The results are shown in Fig. 13 and prove clearly that a large number of small droplets in the active biased spray discharge produces a small effective resistance (in the order of $6 \times 10^9 \Omega$ and lower) and indicate that the active spray method represents the most promising approach.* The discharge from 20 kV to 0 V took only 11 seconds and needed only 0.3 lb water.

The passive spray discharge without bias yields an effective resistance of $3.3 \times 10^{10} \Omega$ which is only twice as large as the effective resistance demonstrated with the standard nozzle at 10 ft height using 8.7 lb of water. However, during this passive spray experiment, only 1.33 lb were used for a discharge from 20 kV to 2 kV within 34 seconds.

There is a basic difference between the active spray with small droplets and large droplets in the selection of the bias polarity. In contrast to the large droplet case, a bias polarity between bias ring and nozzle is required that is opposite to the polarity between fuselage and ground. Physical details of the biased discharge as a function of droplet size and density distribution require further fundamental investigations.

4. ELECTRIC FIELD SENSING

Equally significant as the discharge problem itself, is the magnitude and polarity of the potential between the cargo hook and the ground. The two following methods have been considered for sensing of the electrostatic field between the helicopter and ground as a means to determine this potential:

*Laboratory experiments showed that a single spray nozzle can produce a discharge current in excess of 10 μ A under optimized conditions.

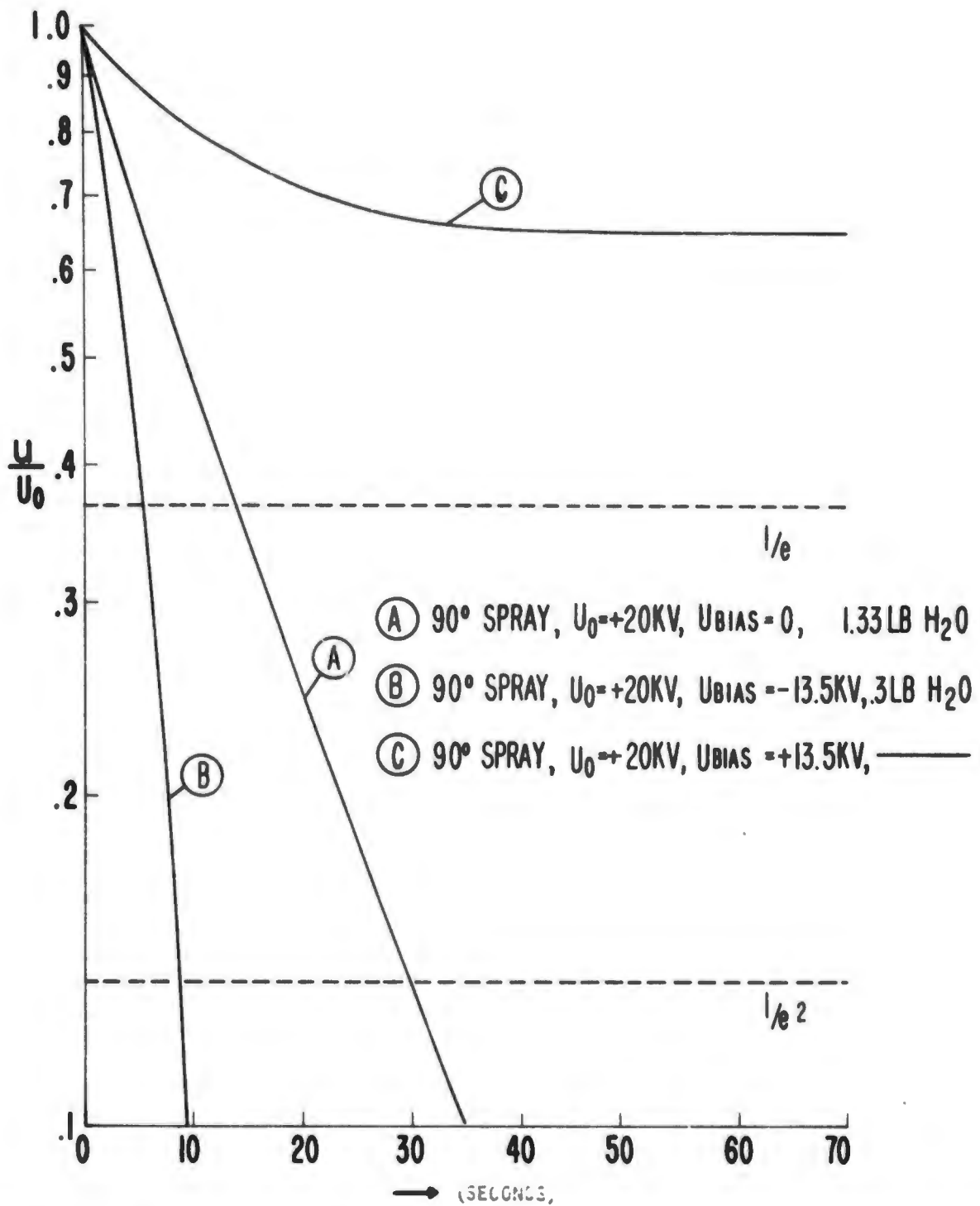


FIG.13 EFFECT OF BIASED ELECTRODE ON SPRAY DISCHARGE RATE

4.1 Corona Discharge Noise Indicator

As a body charges, a concentrated electric field is produced at sharp points and extremities. Eventually, the field at those points becomes sufficiently large to go into burst pulse corona. This type of corona was first investigated by Mr. Trichel in 1938.⁷ These pulses of ms duration have a short rise time, and occur at nearly periodic frequencies.⁸ This induced noise may be used as a measure of the charge the helicopter carries for defined discharge tip conditions. Preliminary laboratory experiments indicate that above 5000 V this method is indeed feasible.⁹ Considering the fact that it may be possible to use in part the existing communication gear within the helicopter, this approach may be indeed very simple and inexpensive. The results obtained so far, however, have to be refined.

4.2 Electrostatic Field Sensing Methods

A different method, which has been studied in some detail, is a modernization and miniaturization of the classical "field mill" which works according to the following principle:

A homogeneous electric field E , induces in a plate of area A , an opposing positive and negative charge $q = A \epsilon_0 E$. For example, with $A = 1 \text{ cm}^2$, $\epsilon_0 = 8.86 \times 10^{-14} \text{ coulomb/Vcm}$, and $E = 10 \text{ V/cm}$ (for a helicopter potential of 3000 V at 10 ft height), q becomes 8.86×10^{-13} coulomb. This charge causes a voltage u_0 at the input electrode of the probe amplifier equal to q/C_i . With a total amplifier input capacity $C_i = 20 \times 10^{-12} \text{ F}$, we obtain a dc signal of 44 millivolts controlling either the grid of an electrometer tube or the gate of a MOSFET, depending on the device choice for the amplifier input. This initial voltage u_0 , tends to decay across the input resistance R_i (typical values for R_i in the order of $10^{12} \Omega$ can be attained without sacrifice in amplifier stability). The instantaneous voltage u , of this decay is $u = u_0 \exp(-t/\tau)$ where the time constant $\tau = R_i C_i = 20$ seconds. If the probe is periodically shielded for relatively short intervals $t_s - t_e$ in comparison to the exposure intervals t_e (where t_r represents the exposure repetition period), then the charge distribution on the probe induced by exposure to the field collapses and the amplifier signal u returns to zero. Furthermore, if this field

exposure repetition time is $t_r \leq .1 \tau_i$, then the amplifier input voltage stays nearly constant $\bar{u} \approx u_0$ during pulses of the length t_e . With integrating RC networks following the probe amplifier having a voltage gain G, an average output voltage \bar{u} , proportional to the probed electrostatic field strength is available at the amplifier output

$$\bar{u} = G u_0 \frac{t_e}{t_r} = \frac{G A \epsilon_0 E t_e}{C_i t_r}$$

The repetitive probe exposure may be accomplished in several ways.

a. A rotating blade alternately exposes the probe and shields it from the unknown electrostatic field.¹⁰ This approach has been experimentally demonstrated in a preliminary experiment. However, the single electrometer tube used for this experiment did not exhibit sufficient linearity between the applied electrostatic field and the output reading, nor did it exhibit a sufficient agreement between outputs when the polarity of a given field strength was changed. These deficiencies could have been eliminated by including the electrometer tube into the negative feedback loop of a successive high gain integrated operational amplifier.

b. An electromagnetically driven shutter or relay contact, located above the field sensing probe, exposes or shields the probe alternately while a short between probe and probe case is applied during the period of probe shielding. Recently, a similar device has become commercially available from Enviro/Tech Sciences and has been successfully tested.

It is possible to attach a detector of this kind reduced to the size of a flashlight (including battery and a small telemetric system) to the cargo hook. However, the problem of protection, reliability, and field distortion still needs further consideration.

c. Another method is the Inverted Van der Graaff apparatus.¹¹ A high voltage generator belt made from an insulating material. This belt transports these charges into a metallic sphere acting as Faraday cage, where they are collected by brushes in order to increase the potential on the sphere surface. This concept can be converted to operate as a charge detector if the following changes are made. The metal sphere must be incorporated into the lower extremities of the helicopter to assume the proper charge density. Charges on the sphere surface must be transported

through an opening into the sphere cavity to the input terminal of a sensitive dc amplifier located inside. This charge transport can be accomplished with a mechanism operating a probe electrode that periodically appears on the sphere surface, moves inside the sphere and discharges into the effective capacitance of the dc amplifier input. The output level of the dc amplifier is then proportional to the helicopter charge and can control a fluid discharge from the helicopter. The term "inverted Van der Graaf" has been coined to indicate charge depletion rather than charge generation on the sphere. As yet, no experiments have been conducted to implement this inverted Van der

5. INFORMATION PROCESSOR/INDICATOR

After field strength and field polarity is determined by the probe, the information must be evaluated and processed to initiate the discharge mechanism and steer the indicator lights. In our experimental system, the signal at the output of the probe amplifier stages still consists of pulses proportional to the strength of the electrostatic field sensed during the exposure periods. The polarity of these pulses corresponds to the direction of the measured field. In the W 100 field probe,* for example, these pulses range typically from +2.5 V to -2.5 V for full scale meter deflection in both polarities. The dynamic range of the field probe can be adjusted to span the maximal expected helicopter potential range at hovering height by probe gain adjustment. If for example, the aircraft is considered "safe" at potentials below 2 kV absolute, the probe output pulse level could range from +0.25V to -0.25V for the "safe" region (assuming an electric field below 700 V/m). This is considered a reasonable threshold range to initiate the corresponding digital information processing by driving the input of the lab designed discharge control circuitry shown in Fig. 14. The input pulses are amplified with a Fairchild type μ A 741 integrated linear operational amplifier wired for a closed loop gain adjustable with the threshold control from 4.4 to 22. If the discharge is to be initiated above a 0.25V input magnitude, the threshold control is to be adjusted for a close loop voltage gain near 10.

The center portion of the schematic diagram in Fig. 14 exhibits a symmetry below and above the common ground line. The upper part of this symmetrical portion processes positive pulses and the lower part processes negative pulses coming from the operational

*Calibrated Electrostatic Charge Detector, Model W100, Enviro/Tech Sciences, Inc., Newton Upper Falls, Mass., modified in the labs to match the application requirements.

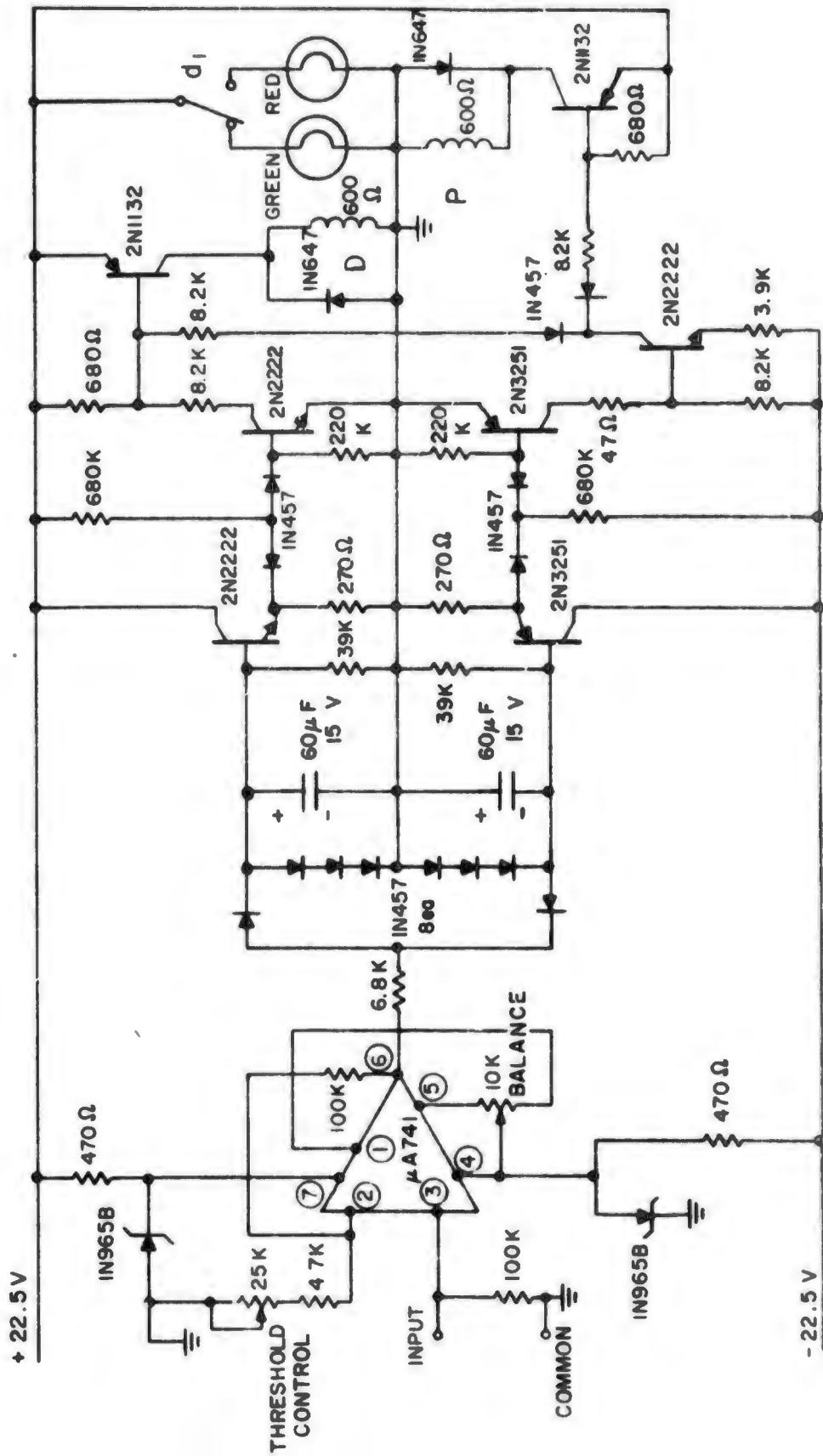


FIG.14 CIRCUIT DIAGRAM OF THE SIGNAL SENSOR TRIGGERED DISCHARGE CONTROL

amplifier output. The network, consisting of eight silicon diodes, separates these output pulses by polarity and limits their magnitude regardless of polarity to 2.1 V (3 diode drops) across either charging capacitor.

The 0.5 second gaps between the 2.5 second pulses (typical for the W 100 probe) are filled in by charge storage in either $60\mu\text{F}$ capacitor, each discharging into a $39\text{ K}\Omega$ resistor in the absence of a signal with a time constant of approximately 2.4 seconds. Two emitter follower stages, one for each polarity, function as impedance transformers and sink the current from the following diode-transmitter logic (DTL) stages. Subsequently, either DTL transistor can actuate the discharge control relay D, and the DTL transistor for negative going pulses can also control the nozzle bias reversal relay P. One of the following situations exists for an operational amplifier gain of 10:

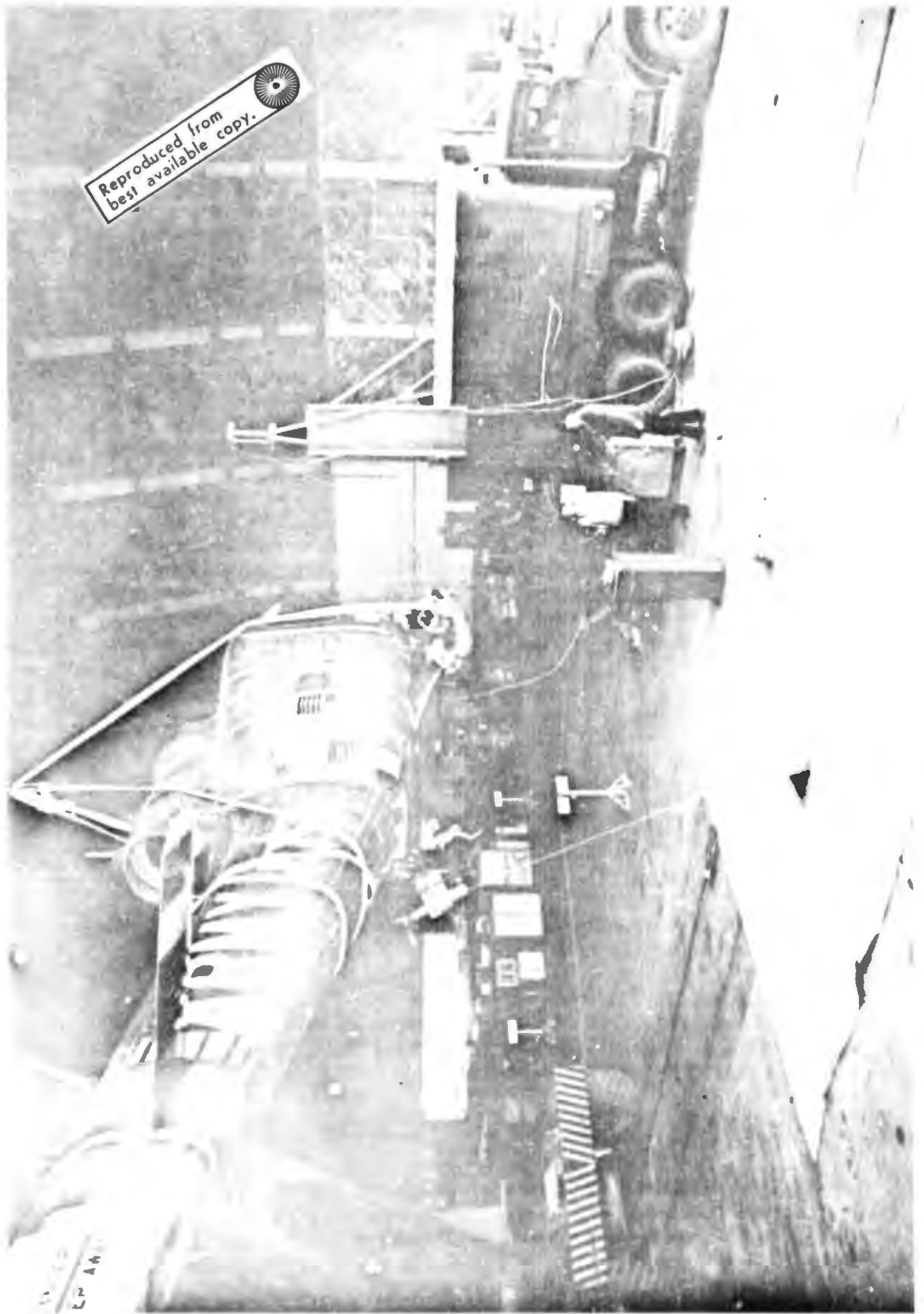
a. For input levels above $+0.25\text{ V}$, the NPN emitter follower raises the voltage across the 270Ω resistor above 1.4 V , and a base current will flow into the NPN DTL transistor which triggers the driver for relay D and initiates a fluid discharge with the proper bias polarity while the red warning light is on.

b. For input levels below -0.25 V , the Si-PNP emitter follower causes the voltage across the 270Ω resistor to go below -1.4 V ; as a result, the Si-PNP DTL transistor becomes conductive and triggers the driver for relay D and the driver for relay P. This initiates the discharge with the opposite bias polarity while the red warning light is on.

c. At input levels between $\pm 0.25\text{ V}$, neither emitter follower produces a voltage magnitude above 1.4 V across either 270Ω resistor and no DTL transistor can conduct as neither base is driven. The green safety light indicates a safe helicopter potential.

6. OVERALL SYSTEMS TESTS

The general concept of an overall system that encompasses field sensing and active discharge system with information receiver and processor has been shown in Fig. 1, and a photograph of the actual setup is presented in Fig. 15. Before the current version of the discharge control, as shown in Fig. 14, was completed, an earlier and simpler circuitry sensitive only to positive helicopter potential against ground was used to test this overall systems concept. For optimum W 100 probe location within the electrostatic field between



SUSPENDED FUSELAGE

FIG.15

fuselage and ground, a battery operated and laser triggered winch was designed, built, and mounted onto the fuselage. The miniature hoist motor was controlled by a digital circuitry that changed to the appropriate up, down, or stop mode when one of three corresponding photosensitive resistors mounted near the control box were laser illuminated. The entire circuitry, shown in Fig. 4, is needed to control the hoist motor (while the dual-sensor portion on this circuit is sufficient for laser beam control of the vacuum contactors).

During these preliminary systems tests, using single polarity sensing only, it was demonstrated that the field initiated helicopter discharge works well with passive and active discharge systems. The repetition of the experiment with polarity independent field sensing and active discharge spray is scheduled for the near future. Later on, the field sensor will be mounted as a separate and independent package on the cargo hook and linked with the remaining portions by radio control rather than by direct line connection, as in the present setup. The discharge control circuitry, shown in Fig. 14, will be expanded, using a radio receiver at the input, and the probe unit will be equipped with a simple telemetry transmitter. The carrier will be modulated proportional to the level and polarity of the probe output pulses.

7. FUTURE EXPERIMENTS

There are several subjects which will be explored in FY-72 if funds become available.

- a. Further laboratory experiments will be performed which permit a more reliable basis for optimization of the active discharge system. Most efforts will be devoted to multiple spray nozzle arrays.
- b. Major emphasis will be on a sequence of test flights to study performance of system elements under actual field conditions.
- c. An effort will be made to characterize extreme operational conditions in severe dust or snow environments. Very little is known in this area and the existing requirements are only derived from a scaling of experiments from smaller helicopters.
- d. Experiments will be conducted to assess the merits of the inverted Van der Graaff concept.
- e. The drop density and size distribution for the various fluid discharges will be investigated experimentally in order to optimize individual nozzle designs for maximum discharge current per unit discharge fluid.

8. SUMMARY

a. Feasibility of the dielectric discharge for the purpose of discharging a helicopter has been established in passive and active mode operation within the present limitations discussed in this report.

b. Miniaturized solid state circuitry has been developed in breadboard form for field sensing and for appropriate information processing.

c. All preliminary systems elements have been tested separately and as a unit.

9. ACKNOWLEDGEMENTS

All parts of the program were performed in close cooperation with and supported by the Avionics Laboratory, ECOM; valuable technical comments and extremely competent administrative support are due to Mr. H. Inslerman, whose numerous services provided an excellent contact with the Avionics Laboratory.

10. REFERENCES

1. H. E. Inslerman, R. W. Creed, W. C. Barr, R. G. Spicer, "ENSURE 265 CH-54 (Flying Crane) Electrostatic Discharge Evaluation," R&D Technical Report ECOM-3120, April 1969.
2. I. H. Inslerman, "Resistive Link Portions of Safe Cargo Hook-up Systems," R&D Tech Report ECOM 02412-6, PPAR Contract DA 28-043-AMC-02412(E), September 1970.
3. R. G. Buser, H. Kaunzinger, H.E. Inslerman, "Discharge of Helicopters by Electronically Controlled Emission of Charge Carrying Liquid Droplets," Army Science Conference Paper, 2 March 1972.
4. USAECOM Safety Regulations ESC-FM 3428-66 list hazardous currents:
 - 0.01A - painful
 - 0.03A - severe shock
 - 0.1 to .2A - lethal (ventricular fibrillation of the heart)
5. R. G. Buser, H. Kaunzinger, USAECOM Invention Disclosure Docket No. 0030 "Electrostatic Discharge by Charge Droplet Emission from Biased Nozzle Array," 30 July 1971.
6. H. D. Bowen, P. Hebblethwaite, W. M. Caleson, "Application of Electrostatic Charging to the Depositing of Insecticides and Fungicides on Plant Surfaces," Agricultural Engineering, p. 347, June 1952.
7. G.W. Trichel, "The Mechanism of the Negative Point to Plane Corona Near On-Set," Phys. Rev., Vol. 54, p. 1078, 15 December 1938.

8. R. L. Tanner, "Radio Interference from Corona Discharges," Technical Report No. 37, SRI Proj. 591, Air Force Contract No. AF 19 (64)-266, 1953

9. R. G. Buser, H. Inslerman, W. Berndt, H. Kaunzinger. USAECOM Invention Disclosure Docket No. 0031 "Electrostatic Charge Indication and Discharge Control Using Corona Noise," 2 August 1971.

10. H. Kaunzinger, R. Buser, USAECOM Invention Disclosure Docket No. 0029 "Electronic Version of the Field Mill Concept," 30 July 1971.

11. R. G. Buser, H. Kaunzinger, USAECOM Invention Disclosure Docket No. 0105 "Inverted Van der Graaff Apparatus," 30 September 1971.